Biosensors and Bioelectronics 56 (2014) 307–312

Contents lists available at ScienceDirect

Biosensors and Bioelectronics

journal homepage: www.elsevier.com/locate/bios

Low-toxic Ag_2S quantum dots for photoelectrochemical detection glucose and cancer cells

Xiaoru Zhang [a], Mingshuai Liu [a], Hongxia Liu [a], Shusheng Zhang [a,b,*]

[a] Key Laboratory of Sensor Analysis of Tumor Marker, Ministry of Education, College of Chemistry and Molecular Engineering, Qingdao University of Science and Technology, Qingdao 266042, PR China

[b] Key Laboratory of Detection Technology of Shandong Province for Tumor Marker, College of Chemistry and Chemical Engineering, Linyi University, Linyi 276005, PR China

ARTICLE INFO

Article history:
Received 9 December 2013
Accepted 17 January 2014
Available online 23 January 2014

Keywords:
Photoelectrochemical biosensor
Ag_2S quantum dots
Glucose
Cancer cell

ABSTRACT

A new photoelectrochemical (PEC) biosensor was developed using low-toxic Ag_2S QDs as photoelectrochemically active species. Energy levels of Ag_2S and Ag_2Se QD were compared to explain their differences in the PEC performance. The preparation condition of Ag_2S QD was optimized and its structure characterization was measured. Then the developed photoelectric active interface was used to detect glucose and MCF-7 cancer cell and showed the good sensitivity and specificity. Under optimal condition, detection limits of 3.2×10^{-5} M for glucose and 98 cells/mL for MCF-7 cell were achieved. Thus, the prepared Ag_2S QD could serve as an excellent and promising photoelectric active material in the PEC biosensor.

1. Introduction

Photoelectrochemical detection is a new and promising analytical technique for a biological assay. Due to its separate source for excitation and detection, the sensitivity of the photoelectrochemistry (PEC) based analytical method can potentially match that of the electrochemiluminescence (ECL) (Zhang et al., 2013; Qian et al., 2010). The usually used photoelectrochemically active species are rutheniumbipyridine derivatives (Liang et al., 2008; Liang and Guo, 2007), semiconductor nanostructures (such as CdSe/CdS, TiO_2 and ZnO) (Wang et al., 2009a; Sun et al., 2008, 2014) and dyes (Ikeda et al., 2009; Hu et al., 2013). Among them, semi-conductor nanoparticles (NPs) have attracted much attention, due to the unique size- and shape-dependent optical and electronic properties.

However, it is well known that the ZnO NPs suffer from their instability. As a result of significant photoelectrochemical materials semiconductor, TiO_2 NPs have gained much attention in photoelectrochemical solar cells. Bare TiO_2 is a wide band gap semiconductor material and is photoelectrochemically active under UV irradiation (Wang et al., 2009b). But the destructive effect of UV light and the strong oxidation power of the photoholes of TiO_2 limit its application in the PEC biosensor (Tachikawa et al., 2011; Yan et al., 2013). CdS and CdSe quantum dots (QDs) are narrow band gap semiconductor materials, which are photoelectrochemically active in the visible range and have been widely used in photoelectrochemical sensors. The most challenging aspect of working with Cd-based probes in biological systems, however, is related to its toxicity that can result from the decomposition and release of heavy metal ions (Sun et al., 2013). So, they might be toxic to cells if used for in vitro characterization of cell cultures, and if used for diagnostic test, the particles might be a hazard to the technician carrying out an assay. Therefore, there is an urgent demand to develop Cd-free nanoparticles for bio-applications.

With a narrow band gap and low toxicity, nanoscale Ag_2S and Ag_2Se are potential candidates for near infrared (NIR) QDs, which are desirable for the use of imaging in vivo (Jiang et al., 2012; Sahu et al., 2011; Gu et al., 2012). At the same time, the small Ag_2S and Ag_2Se QDs have enormous surface area-to-volume ratios, which may be highly susceptible to heterogeneous redox chemistry with surrounding environments. Recently, Pang's group has reported ECL behaviors of Ag_2Se QDs at the multiwalled carbon nanotubes (MWCNTs) and polyethyleneimine (PEI) modified glassy carbon electrode (GCE) (Cui et al., 2012).

In this work, we synthesized Ag_2S and Ag_2Se QDs and then investigated their application in the PEC biosensor for the first time. The result shows that the performance of Ag_2S QD is much better than that of Ag_2Se QD. After optimization of reaction condition and investigation of its optoelectronic properties, the obtained Ag_2S QD was assembled on an ITO electrode and used as an optoelectronic platform. Then, glucose and cancer cell MCF-7 were selected as PEC detection targets to demonstrate the application prospect of Ag_2S QD in the field of PEC biosensor.

* Corresponding author at: Linyi University, College of Chemistry and Chemical Engineering, Key Laboratory of Detection Technology of Shandong Province for Tumor Marker, Linyi 276005, PR China. Tel./fax: +86 532 84022750.
E-mail address: shushzhang@126.com (S. Zhang).

0956-5663/$ - see front matter © 2014 Elsevier B.V. All rights reserved.
http://dx.doi.org/10.1016/j.bios.2014.01.033

2. Experiment

2.1. Materials and apparatus

2.1.1. Materials

3-Mercaptopropionic acid (3-MPA), BSA, sialidase, glucose oxidase (GOx) and 1-ethyl-3-(3-dimethylaminopropyl) carbodiimide hydrochloride (EDC·HCl) were purchased from Sigma. Ascorbic acid (AA) and sialic acid (SA) were obtained from Aladdin. N-hydroxysuccinimide (NHS) and 3-APBA (3-aminophenylboronic acid) were purchased from J&K Scientific. Silver nitrate ($AgNO_3$) was obtained from Sinopharm Chemical Reagent Co., Ltd. Sodium sulfide (Na_2S), acetic acid (CH_3COOH), sodium hydroxide (NaOH) and glucose were purchased from Tianjin Bodi Chemical Co., Ltd. (China). All other chemicals were of analytical grade and used without further purification. All solutions were prepared with doubly distilled water (DDW). MCF-7 cell was obtained from Chinese Academy of Medical Sciences.

2.1.2. Apparatus

The photocurrent was measured on an electrochemical workstation (Zahner Zennium, Germany). A three-electrode system was employed with a Pt wire as an auxiliary electrode, Ag/AgCl as a reference electrode and an ITO conductive glass supplied by China Southern Glass Holding Co., Ltd. (Shenzhen, PR China, ITO coating 180 ± 25 nm, sheet resistance $\leq 10\ \Omega$/sq) as a working electrode. A SEM (JSM-7500F, JEOL Ltd., Japan) was used to examine the morphology of Ag_2S QDs. A TEM image was observed on a JEM-2100 transmission electron microscope (JEOL Ltd., Japan). UV/vis spectra were carried out on a Cary 50 UV/vis–NIR spectrophotometer (Varian). Cyclic voltammetry curves were observed on a CHI-832B electrochemical workstation (Shanghai Chenhua Apparatus Corporation, China). Steady-state photocurrent response was observed on a MPI-EO photoelectrochemical workstation (Xianruimai Analytical Instruments Co., Ltd., China).

2.2. Preparation of Ag_2S QD

Ag_2S QD was synthesized according to the procedure of literature with a slight modification (Hocaoglu et al., 2012). Briefly, 15 mL DDW was added into a 50 mL three-necked flask. After bubbling with N_2 for 20 min, 3-MPA was added. The pH of the solution was adjusted to 7.5 using 2 M NaOH and 2 M CH_3COOH solutions. 0.05 mmol $AgNO_3$ was added, the pH was readjusted to 7.5 and the reaction mixture was stirred at (56 °C, 75 °C, 90 °C and 110 °C) for 5 min. Then, 5 mL of deoxygenated aqueous Na_2S solution was added slowly through a syringe and the color changed to yellow. The reaction mixture was heated under vigorous stirring until the end of the reaction. For purification, the obtained brown solution (20 mL) was mixed with 20 mL acetone and centrifuged at 3000 rpm for 5 min. Then the precipitation was washed with DDW and the process was repeated three times. The obtained precipitation was dissolved in 0.01 M of NaOH (20 mL) and stored at 4 °C in dark after ultrasonic dispersion.

2.3. Preparation Ag_2Se QD

Ag_2Se QD was prepared as described with a slight modification (Chen et al., 2013). Simply, 20 mL DDW was added into a small flask. Then 0.40 g selenium and 1.0 g $NaBH_4$ were added under nitrogen atmosphere with continuous stirring. When black selenium disappeared after 40 min, the reaction mixture was cooled with ice-water until a white precipitate was obtained. After centrifugation, a solution of NaHSe (0.25 mol/L) was obtained for later use.

0.009 mmol $AgNO_3$ and 0.036 mmol GSH were dissolved in 20 mL DDW and stirred under nitrogen atmosphere for 30 min. The pH of mixture was adjusted to 9.5 using 2.0 mol/L NaOH and 2.0 mol/L CH_3COOH. After raising the temperature to 85 °C, 25 μL 0.25 mol/L NaHSe prepared previously was added and the mixture was stirred at 85 °C for 2 h to give a light brown solution.

2.4. Preparation of SnO_2 modified ITO electrode

An SnO_2 electrode was prepared according to literature (Liang et al., 2006). Briefly, an ITO-coated glass was cleaned in an ultrasonic cleaner with each of the following solutions sequentially: household detergent in water (15 min), deionized water (2 min, twice), acetone (5 min), 2-propanol (5 min), and deionized water (10 min, twice). Tin (IV) oxide (10%) was spread on a piece of ITO-coated glass and then dried in air. The film was then sintered at 450 °C for 60 min and the semiconductor thin films were adhered strongly to the glass surface.

2.5. Preparation of GOx modified electrode and the detection of glucose

10 μL of the Ag_2S QDs stock solution was coated onto a piece of SnO_2 modified ITO electrode and dried at room temperature. The resulting Ag_2S/SnO_2/ITO electrode was activated by casting the mixture of 5 μL EDC·HCl,25 mM,and NHS,25 mM, for 15 min. Then 5 μL 0.2 mg/mL GOx solution was casted onto the assembled electrode surface for the conjugation of the primary amine groups of GOx to the carboxyl groups of Ag_2S QDs. After incubating at room temperature for another 2 h, the Ag_2S/SnO_2/ITO electrode was thoroughly rinsed with DDW, dried under nitrogen atmosphere and stored at 4 . During PEC detection for glucose, 0.1 M Tris–HCl was employed as a supporting electrolyte.

2.6. Preparation of benzeneboronic acid modified electrode and the detection of cell MCF-7

Ag_2S/SnO_2/ITO electrode obtained above was activated by casting 5 μL mixture of EDC·HCL,25 mM,and NHS,25 mM,and incubated for 15 min. Then 5 μL 3-APBA (25 mM) was casted onto the assembled electrode surface for the conjugation of the primary amine groups of 3-APBA to the carboxyl groups of Ag_2S QDs. After incubating at room temperature for another 2 h, the Ag_2S/SnO_2/ITO electrode was thoroughly rinsed with DDW and dried under nitrogen atmosphere. The assembled electrode was blocked with 10 μL 2% BSA at room temperature for another 1 h, then washed with 2% Tween 20, DDW and dried under nitrogen atmosphere. Finally, the modified electrode was immersed in 500 μL of cell solution and incubated at 37 °C for 60 min followed by washing with buffer solution before measurement. During PEC detection for cells, 0.1 M PBS was employed as a supporting electrolyte.

All experiments were repeated at least five times and the means of measurements were presented with the relative standard deviations unless otherwise stated.

3. Results and discussion

3.1. Photoelectric performance of Ag_2S and Ag_2Se

The photoelectric performances of Ag_2S and Ag_2Se were investigated in order to choose the better one in the PEC biosensor. As shown in Fig. 1A, when Ag_2S is immobilized on ITO/SnO_2 electrode, the photocurrent is about 1650 nA (curve a). But when

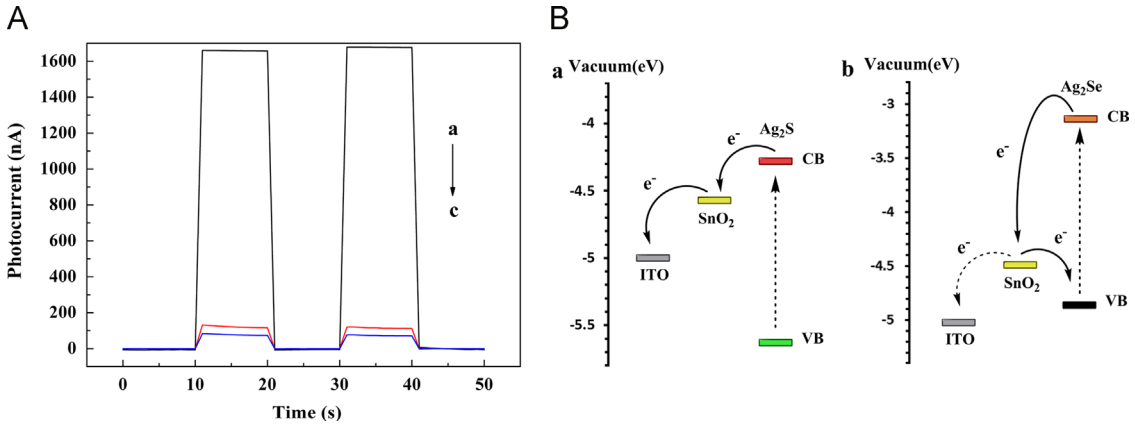

Fig. 1. (A) Photocurrent of electrode (a) ITO–SnO_2/Ag_2S QD; (b) ITO–SnO_2/Ag_2Se QD; and (c) ITO/Ag_2S QD. (B) Energy-level diagram of (a) Ag_2S QD and (b) Ag_2Se QD.

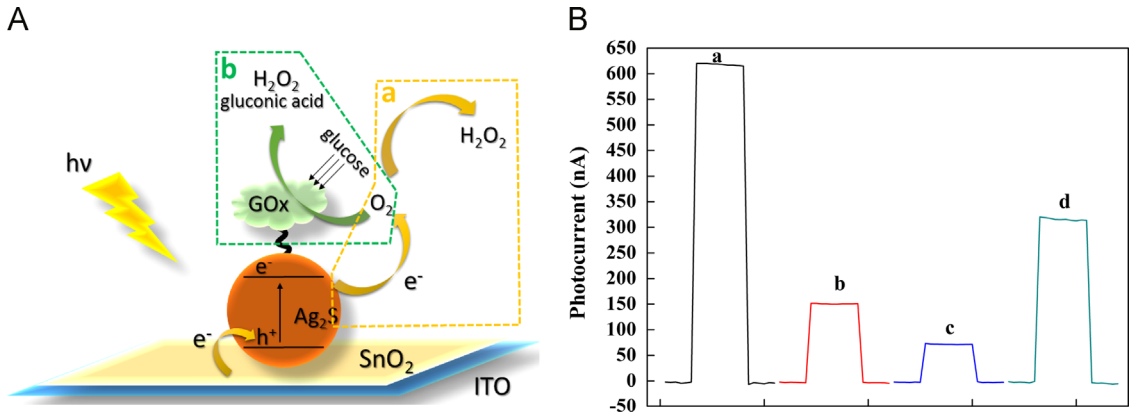

Fig. 2. (A) Schematic illustration for the detection of glucose at GOx/Ag_2S/SnO_2/ITO electrode. (B) Photocurrent responses of GOx/Ag_2S/SnO_2/ITO electrode in air-saturation (a), N_2-saturation with 400 μM H_2O_2 (b), N_2-saturation (c), and air-saturation with 10.2 mM glucose (d).

Ag_2Se is immobilized on the same electrode, the photocurrent is only 160 nA (curve b). In addition, comparing curve a and curve c, we find that the coating of SnO_2 on ITO electrode could enhance the photoelectric performance greatly. All these can be explained as follows.

For Ag_2S QDs, cyclic voltammetry and the optical absorption spectrum were used to determine the LOMO level and band-gap value (Cui et al., 2012; Zhao et al., 2012). From the results of Fig. 1B, LUMO and HUMO for Ag_2S QD are −4.25 eV and −5.63 eV, respectively (see Figs. S1 and S2 in supplementary material), while SnO_2 has a work function of about −4.5 eV (Tiwana et al., 2012). So, electron-transfer from the conduction band (CB) of Ag_2S QD to SnO_2 was an energetically favorable process. The work function of ITO (−5.0 eV) (Zhao et al., 2012) further facilitated the electron-transfer from SnO_2 to ITO, thereby leading to the generation of a photocurrent (Fig. 1B(a)). Using the same method, we could deduce that the LUMO and HUMO for Ag_2Se were −3.15 eV and −4.86 eV, respectively. Thus, after electron-transfer from the CB of Ag_2Se QD to SnO_2, the electron-transfer from SnO_2 to the VB of Ag_2Se had priority over the ITO electrode (as shown in Fig. 2B(b)) and led to electron–hole recombination of excited Ag_2Se QD. Accordingly, the photocurrent produced by Ag_2Se QD was much lower than that produced by Ag_2S QD.

3.2. Condition during PEC measurement

As for the ITO electrode assembled with both SnO_2 and Ag_2S, the photocurrent response changed with the excitation wavelength, and reached its peak at about 400 nm. While for the ITO electrode assembled with SnO_2 alone, the photocurrent was much lower regardless of the excitation wavelength (Fig. S3A in supplementary material). It is also worth mentioning that the photocurrent response for Ag_2S/SnO_2/ITO electrode was fairly reversible and stable under several on/off irradiation cycles for 240 s (Fig. S3B in supplementary material). Thus, it could be used as a detection signal. PEC detection was carried out in 0.1 M PBS (pH=7.4) containing 0.1 M AA (Fig. S4 in supplementary material), which served as a sacrificial electron donor during the photocurrent measurement.

3.3. Condition during preparation of Ag_2S QD and its crystal structure character

The photoelectro-activity can be tuned with Ag:S ratios, ligand: Ag ratios, reaction temperature and reaction time. Through comprehensive investigation and comparison shown in Fig. S5B of supplementary material, the best photoelectro quality of Ag_2S QD is obtained when reaction is performed at 90 °C for 3 h, Ag:S ratio of 6 and 3-MPA:Ag ratio of 5.

The scanning electron microscope (SEM) images (Fig. S6A of supplementary material) gave us a whole view of the morphology and size of the samples. Transmission electron microscopy (TEM) image of a typical Ag_2S QD sample is shown in Fig. S6B of supplementary material. The nanocrystals were nearly monodispersed with an average size of ca. 10 nm. Energy dispersive X-ray spectroscopy (EDX) characterization (Fig. S6C of supplementary material) of the purified products proved that the products were composed of Ag and S elements with appropriate stoichiometry of bulk Ag_2S. This evidence unambiguously illustrates the pure phase of the as-obtained Ag_2S QD. The size distribution histogram

obtained by measuring the diameter of several hundred particles showed a narrow size distribution for synthesized Ag_2S QD (Fig. S6D of supplementary material). Zeta potential showed that the prepared Ag_2S QD was electronegative (Fig. S7 in supplementary material).

3.4. Detection of glucose

The fabrication of glucose biosensor was simple and is shown in Fig. 2A. It was reported that oxygen was sensitive to the PEC biosensor, and it could act as an electron acceptor during the photoelectrochemical process and produced cathodic photocurrent (Wang et al., 2012). This can be confirmed by curve a of Fig. 2B. The photocurrent density of Gox/Ag_2S/SnO_2/ITO electrode was about 620 nA in air-saturated buffer under light irradiation with wavelength of 430 nm. After bubbling nitrogen for about 30 min, an obvious decrease in the photocurrent intensity was observed due to the exclusion of oxygen (70 nA, curve c). So, oxygen acted as an electron acceptor during the PEC measurement. After adding 400 μM hydrogen peroxide to nitrogen saturated solution, the photocurrent increased to only 150 nA (curve b). This indicated that oxygen was more efficient than hydrogen peroxide during the PEC test. When the electrode was exposed to a solution containing glucose, the covalently attached GOx could catalyze the conversion of glucose into gluconic acid and hydrogen peroxide with the consumption of dissolved oxygen, thus causing the depression in photocurrent. As shown in curve d of Fig. 2B, after adding 10.2 mM glucose, the photocurrent decreases to about 315 nA. In this way, we could realize the detection of glucose. Further, if GOx was immobilized on antibody, we could expand the range of detectable targets by using the sandwich assay in measuring protein biomarkers.

The pH value has a large effect on the PEC detection. When the pH becomes alkaline, OH^- may attack Ag^+ on the surface of QDs, thus hindering the electron transfer from QDs to O_2 (Wang et al., 2012). The pH values of the system were studied in the range 6.0–9.0 (see Fig. S9 of supplementary material) and Tris–HCl buffer with pH 7.0 was selected for the detection of glucose.

Fig. 3A depicts the photocurrent change of the PEC biosensor in the presence of different concentrations of glucose. As the concentration of glucose increased, photocurrent decreased accordingly. The quantitative behavior of the PEC biosensor was assessed by measuring the dependence of the decreased photocurrent intensity (ΔI) before and after adding different concentrations of glucose. The linear relationship between the photocurrent response and the glucose concentration was observed in the range from 0.1 mM to 12.2 mM (see Fig. 3B). The regression equation was ΔI (nA)$=29.305C_{glucose}+5.006$ (10^{-3} M) with a regression coefficient of 0.9976. A detection limit of 3.24×10^{-5} M could be estimated using 3σ, which was comparable with those of 0.04 mM for CdTe QDs based PEC biosensor (Wang et al., 2012) and 0.1 mM for Langmuir–Blodgett films based amperometric glucose biosensor (Ohnuki et al., 2007).

In order to test the biological application of the proposed method, glucose content in serum sample was investigated. To avoid the deterioration of sample, the serum was freshly diluted with buffer solution before measurement. For comparison, the hexokinase method (spectrophotometry) was also used for determining the samples. Glucose quantities for five different blood samples were determined and summarized in Table S1 in supplementary material. The relative standard deviation was less than 3.8% in five parallel measurements of the same sample.

3.5. Detection of cancer cell MCF-7

The principle of this PEC cytosensor is shown in Fig. 4A. Breast cancer cell MCF-7 is selected as a model cell, as MCF-7 cells overexpress SA on their membrane (Marth et al., 1988; Liu et al., 2013). Monitoring of SA expression on cell surface therefore provides rational indexes of the dynamic changes in tumor malignancy, metastasis and diagnostics. For this purpose, 3-APBA was covalently bounded to the surface of Ag_2S/SnO_2/ITO electrode. Then the interaction between boronic acid and the terminal SA moiety existing on the biological membranes of cells could capture the MCF-7 cell onto this low toxic photoelectric interface. In order to characterize the fabrication process of the PEC biosensor, photocurrent responses at each immobilization step were recorded. As shown in Fig. 4B, the photocurrent for Ag_2S/SnO_2/ITO electrode is about 1650 nA (curve a). When 3-APBA was covalently attached on the –COOH groups of Ag_2S QD (curve b) and blocked with BSA (curve c), the photocurrent decreased slightly. Then the photocurrent decreased obviously after recognition with 3000 cells/mL MCF-7. It could be explained that the immobilization of cell on the electrode surface blocked the diffusion of sacrificial electron donor AA to the surface of electrode and led to the decrease of photocurrent. The results showed that the photoelectron interface made by low toxic Ag_2S QD could be well applied to the detection of bioactive substance.

The pH value may influence the interaction between boronic acid and SA (Matsumoto et al., 2010). Thus the effect of pH on the binding of 3-APBA moieties to SA groups on 3000 cells/mL MCF-7

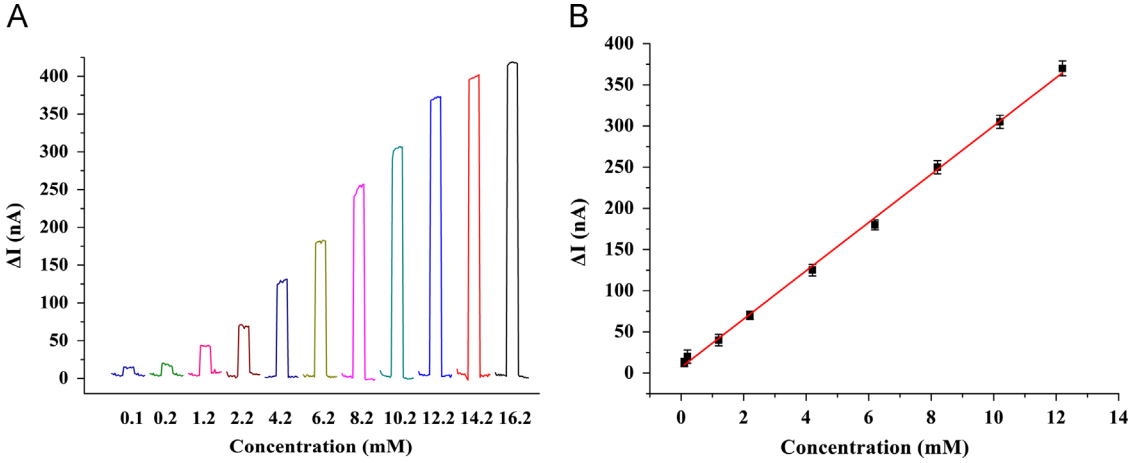

Fig. 3. (A) The decrease in photocurrent towards different concentrations of glucose ($\Delta I=I_0-I$, where I_0 and I are the photocurrents of the GOx/Ag_2S/SnO_2/ITO electrode before and after incubated with glucose, respectively). (B) The calibration curve of the photocurrent decrement versus the concentration of glucose from 0.1 to 12.2 mM. PEC measurement was carried out in 0.1 M Tris–HCl (pH 7.0).

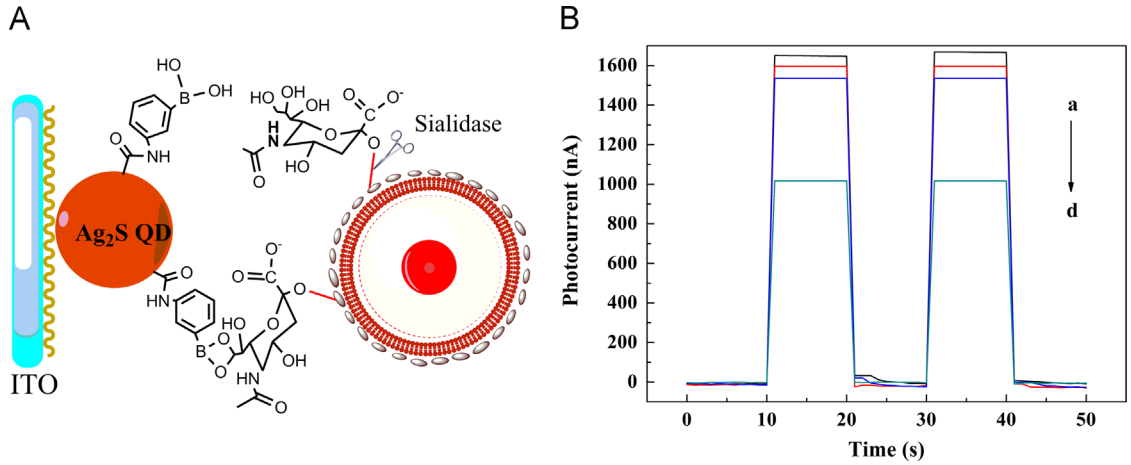

Fig. 4. (A) The PEC cytosensor using 3-APBA modified Ag_2S/SnO_2/ITO electrode and the function of sialidase to remove SA moiety from glycans. (B) Photocurrent responses for (a) ITO/Ag_2S QD; (b) ITO/Ag_2S QD/3-APBA; (c) ITO/Ag_2S QD/3-APBA/BSA; and (d) ITO/Ag_2S QD/3-APBA/BSA/3000 cells/mL MCF-7. PEC measurement was carried out in 0.1 M PBS (pH 7.4) containing 0.1 M AA.

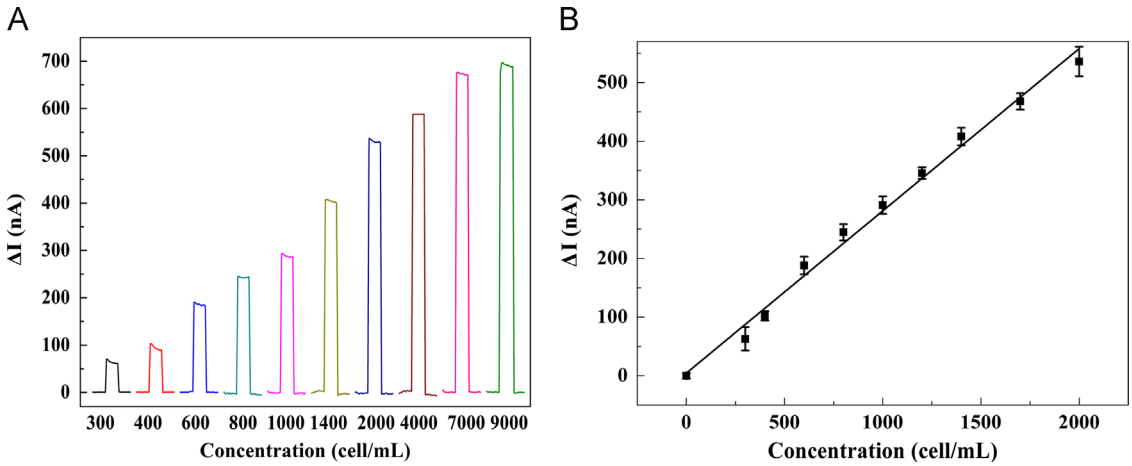

Fig. 5. (A) The decrease in photocurrent towards different concentrations of MCF-7 cells. (B) The linear range of the photocurrent decrement versus the concentration of MCF-7 cell from 300 to 2000 cells/mL.

cells was investigated. As shown in Fig. S10 of supplementary material, the photocurrent increased as the pH changed from 9.0 to 6.5 and boronic acid could form favorable binding with SA on cell surfaces at the physiological pH of 7.4. This result was in good agreement with the previous reports (Han et al., 2011; Otsuka et al., 2003) and physiological pH condition was chosen in later investigation to retain the biological activity of living cells.

The quantitative behavior of the PEC cytosensor was assessed by measuring the dependence of the decreased photocurrent intensity (ΔI) before and after incubating with different concentrations of cells. Fig. 5A shows typical curves of the decreased photocurrent intensity upon concentration of MCF-7 cell. The result indicated that with increasing concentrations of cells, the amount of cells captured on the electrode increased accordingly. Thus, the depression in photocurrent was enhanced. Fig. 5B shows that ΔI increases with increase in concentration of MCF-7 cells ranging from 300 to 9000 cells/mL. The linear range for MCF-7 cell was 300–2000 cells/mL with the equation of ΔI (nA)$=0.277C_{cell}+4.534$ ($R^2=0.9945$, inset of Fig. 5B). A detection limit of 98 cells/mL could be estimated using 3σ, which was comparable with those of 210 cells/mL in fluorescence analysis of BGC cells using boronic acid functionalized QDs (Han et al., 2011) and 84 cells/mL Romas cell for aptamer based PEC cytosensor (Zhang et al., 2011) and much lower than that of 1.0×10^{-3} cells/mL using electrochemical impedance spectroscopy (EIS) for K562 cell (Hao et al., 2007).

To further verify the photocurrent change observed ,which is indeed due to the specific recognition between 3-APBA ligands and cell surface SA, specificity test is performed in Fig. 6A. Free SA (10 mM) was added to the solution of SA overexpressed MCF-7 cell. Comparing the photocurrent obtained from the untreated cell solution (curve a), it was clear that the addition of free SA could effectively inhibit the binding of cell (curve b), indicating that 3-APBA modified electrode had strong binding with SA, while the photocurrent responses for the electrode without modification of APBA were low after treating with the same amount of cell (curve d). In particular, after treating MCF-7 cells with 40 mU mL^{-1} sialidase at 37 °C for 1 h, the decrease of photocurrent was also reduced (curve c). These results verified that our designed platform exhibited specificity to capture sialic acid overexpressed cells. As shown in Fig. 6B, the photocurrent decreases progressively along with the sialidase-treated time, which indicates the decrease of terminal SA on sialidase-treated MCF-7 cells. After treatment with sialidase for 4 h, the SA groups on MCF-7 cells decreased by 82.6%, while the cells exhibited 93% viability after being treated with sialidase for 4 h, indicating favorable cell viability for sialidase treatment (as shown in Fig. S11 of supplementary material).

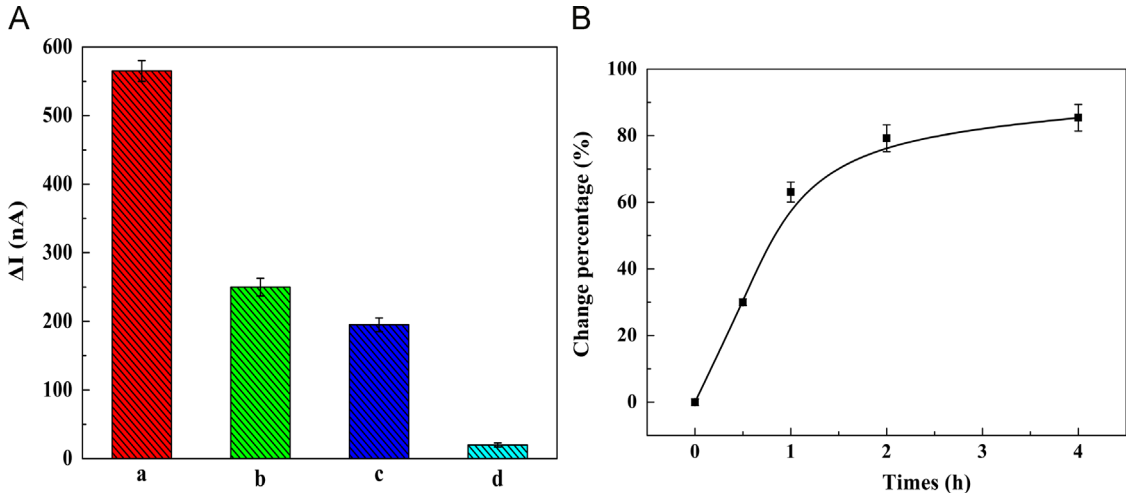

Fig. 6. (A) Photocurrent change (a) after treated with 3000 cells/mL MCF-7 cell; (b) for SA inhibition assay treated with 3000 cells/mL MCF-7 cell solution containing 10 mM SA; (c) for enzymatic reaction treated with 3000 cells/mL MCF-7 cell solution with 40 mU mL^{-1} sialidase at 37 °C for 1 h. (B) Time-dependent photocurrent change for sialidase on SA overexpressive MCF-7 cell (3000 cells/mL). The change percentage (Δ%) was calculated as follows: $\Delta\% = [1 - T/U] \times 100\%$, where T and U are the ΔI obtained on sialidase-treated or untreated cells, respectively.

The toxicity of CdSe and Ag_2S QD was compared in order to prove the low toxicity of Ag_2S QD. First, the viability of MCF-7 cells after being treated with Ag_2S and CdS QDs for different durations was compared (Fig. S12A). After treatment with Ag_2S QDs for 4 h, the cells exhibited 92% viability, indicating favorable cell viability, while after treatment with CdS QDs for 4 h, the cells exhibited only 50% viability. Fig. S12 B shows the viability of MCF-7 cells after exposure at different concentrations of Ag_2S QDs and CdS QDs for 4 h. These observations suggested that Ag_2S QDs almost did not interfere with the cell viability, which was ideal for their use in in vitro and in vivo labeling.

4. Conclusions

In summary, we have prepared a low toxic Ag_2S QD based PEC biosensor for the first time. Instead of conventional CdS or CdSe QD, the Ag_2S QD showed efficient photophysical features without the release of hazardous metal ions. The energy-level-related mechanism of Ag_2S QDs was studied in detail. Glucose and cancer cell MCF-7 were chosen as analyst models to study the potential of Ag_2S QD in the PEC analytical application, which indicated that the prepared Ag_2S QD had extensive potential in the PEC biosensor. So, with its simplicity, low toxicity, sensitivity and wide application range, the Ag_2S QD could become a promising candidate in the PEC biosensor in future.

Acknowledgments

This work was supported by the National Natural Science Foundation of China (Nos. 21275003, 21275086, and 21227008), Excellent Young Scientists Encouragement Foundation of Shandong Province (No. BS2011CL015), and the Program for Changjiang Scholars and Innovative Research Team in University (PCSIRT).

Appendix A. Supplementary material

Supplementary data associated with this article can be found in the online version at http://dx.doi.org/10.1016/j.bios.2014.01.033.

References

Chen, C., He, X., Gao, L., Ma, N., 2013. ACS Appl. Mater. Interfaces 5, 1149–1155.
Cui, R., Gu, Y., Bao, L., Zhao, J., Qi, B., Zhang, Z., Xie, Z., Pang, D., 2012. Anal. Chem. 84, 8932–8935.
Gu, Y., Cui, R., Zhang, Z., Xie, Z., Pang, D., 2012. J. Am. Chem. Soc. 134, 79–82.
Han, E., Ding, L., Ju, H., 2011. Anal. Chem. 83, 7006–7012.
Hao, C., Ding, L., Zhang, X., Ju, H., 2007. Anal. Chem. 79, 4442–4447.
Hocaoglu, I., Çizmeciyan, M.N., Erdem, R., Ozen, C., Kurt, A., Sennarogluad, A., Acar, H.Y., 2012. J. Mater. Chem. 22, 14674–14681.
Hu, Y., Xue, Z., He, H., Ai, R., Liu, X., Lu, X., 2013. Biosens. Bioelectron. 47, 45–49.
Ikeda, A., Nakasu, M., Ogasawara, S., Nakanishi, H., Nakamura, M., Kikuchi, J., 2009. Org. Lett. 11, 1163–1166.
Jiang, P., Zhu, C., Zhang, Z., Tian, Z., Pang, D., 2012. Biomaterials 33, 5130–5135.
Liang, M., Liu, S., Wei, M., Guo, L., 2006. Anal. Chem. 78, 621–623.
Liang, M., Guo, L., 2007. Environ. Sci. Technol. 41, 658–664.
Liang, M., Jia, S., Zhu, S., Guo, L., 2008. Environ. Sci. Technol. 42, 635–639.
Liu, H., Li, Y., Sun, K., Fan, J., Zhang, P., Meng, J., Wang, S., Jiang, L., 2013. J. Am. Chem. Soc. 135, 7603–7609.
Marth, E., Flaschka, G., Stiegler, S., Möse, J.R., 1988. Clin. Chim. Acta 176, 251–257.
Matsumoto, A., Cabral, H., Sato, N., Kataoka, K., Miyahara, Y., 2010. Angew. Chem. Int. Ed. 49, 5494–5497.
Ohnuki, H., Saiki, T., Kusakari, A., Endo, H., Ichihara, M., Izumi, M., 2007. Langmuir 23, 4675–4681.
Otsuka, H., Uchimura, E., Koshino, H., Okano, T., Kataoka, K., 2003. J. Am. Chem. Soc. 125, 3493–3502.
Qian, Z., Bai, H., Wang, G., Xu, J., Chen, H., 2010. Biosens. Bioelectron. 25, 2045–2050.
Sahu, A., Qi, L., Kang, M.S., Deng, D., Norris, D.J., 2011. J. Am. Chem. Soc. 133, 6509–6512.
Sun, W., Yu, Y., Pan, H., Gao, X., Chen, Q., Peng, L., 2008. J. Am. Chem. Soc. 130, 1124–1125.
Sun, B., Zhang, K., Chen, L., Guo, L., Ai, S., 2013. Biosens. Bioelectron. 44, 48–51.
Sun, B., Chen, L., Xu, Y., Liu, M., Yin, H., Ai, S., 2014. Biosens. Bioelectron. 51, 164–169.
Tachikawa, T., Yamashita, S., Majima, T., 2011. J. Am. Chem. Soc. 133, 7197–7204.
Tiwana, P., Docampo, P., Johnston, M.B., Herz, L.M., Snaith, H.J., 2012. Energy Environ. Sci. 5, 9566–9573.
Wang, G., Yu, P., Xu, J., Chen, H., 2009a. J. Phys. Chem. C 113, 11142–11148.
Wang, G., Xu, J., Chen, H., 2009b. Biosens. Bioelectron. 24, 2494–2498.
Wang, W., Bao, L., Lei, J., Tu, W., Ju, H., 2012. Anal. Chim. Acta 744, 33–38.
Yan, Y., Fang, J., Yang, Z., Qiao, J., Wang, Z., Yu, Q., Sun, K., 2013. Chem. Commun. 49, 8632–8634.
Zhang, X., Guo, Y., Liu, M., Zhang, S., 2013. RSC Adv. 3, 2846–2857.
Zhang, X., Li, S., Jin, X., Li, X., 2011. Biosens. Bioelectron. 26, 3674–3678.
Zhao, X., Zhou, S., Jiang, L., Hou, W., Shen, Q., Zhu, J., 2012. Chemistry 18, 4974–4981.